Active Stereo Vision for Autonomous Multirotor UAVs in Indoor Environments

Sven Lange, Peter Protzel
Department of Electrical Engineering and Information Technology
Chemnitz, University of Technology
09111 Chemnitz, Germany
{sven.lange, peter.protzel}@etit.tu-chemnitz.de

***Abstract*— Our work focuses on enabling autonomous navigation in indoor environments without global position information. Ongoing work on a prototypical sensor for range measurements suited to operate on board a quadrotor UAV is presented. Compared to other solutions it is more lightweight, low-cost and able to operate in darkness. Our sensor is based on an active stereo camera utilizing structured light. Results are demonstrated in form of an ICP based localization and an ICP-SLAM application.**

I. Introduction

Our research focuses on enabling autonomous, mobile systems to be applicable in a variety of civil applications, mainly in the areas of emergency response, disaster control, and environmental monitoring. These scenarios require a high level of autonomy, reliability and general robustness from every robotic system, regardless of whether it operates on the ground or in the air.

While the main research interests were focused on mobile ground vehicles over the past years, recently multirotor UAVs became more popular. They are now available in a variety of forms and sizes and can be purchased at affordable prices. The systems can be divided into commercially available systems and open source based UAVs which are often based on the *Mikrokopter* [23] design. Among the commercial systems the ones from AscTec are widely used for research purposes, for instance the *Hummingbird* [11]. In contrast to ground vehicles these UAVs offer greater agility and are independent of the terrain surface quality. Due to their small size they can also be used indoors, which represents a benefit regarding rescue scenarios.

While UAVs work well in environments with available GPS measurements, autonomous navigation without GPS remains a challenge. This is why our research interests are focused on reaching the desired level of autonomy in scenarios where GPS signals are not available. We already developed a method for autonomous landing of our quadrotor system (Fig. 1) [20] and are now working on robust navigation within cluttered indoor environments. We believe this can be done by using a so-called active stereo system consisting of a camera and a structured light source. It is a low-cost and lightweight system which can utilize the already available camera on board the UAV and therefore does not take up much more of the valuable payload.

This work has been funded by the European Union with the European Social Fund (ESF) and by the state of Saxony.

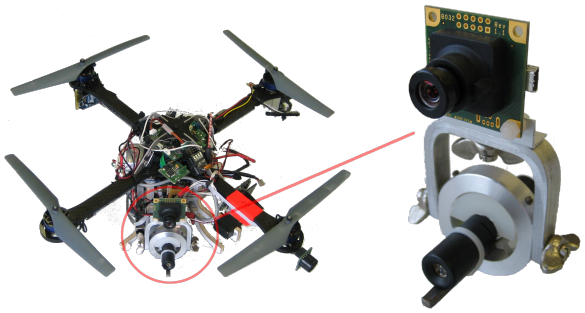

Fig. 1. The image shows our quadrotor system on the left side (an extended *Hummingbird*) and the active stereo vision prototype on the right side. The prototype consists of an IDS uEye color camera (top) and a laser with cylindrical lens for line generation (bottom).

Our goal is to construct a reliable map of the environment including a simplified 3D view detailed enough for a human operator to work with, while using low-cost and lightweight components.

The following section will summarize related work. Afterwards we present the theory of active stereo systems, including calibration and point or line detection procedures. Section IV describes our experience with the simulation environment USARSim. Finally we describe test results based on the acquired measurements of our active stereo camera prototype.

II. Related Work

Different research groups around the world have been working on UAVs for the past years, most of them started with helicopters or aircrafts. They use different kinds of sensor configurations for obstacle detection and achieve autonomous navigation in different environments with lacking GPS signals. Camera based solutions are mainly used in outdoor scenarios. For instance in [2] the authors utilize optical flow sensors extracted from optical mice to detect and avoid obstacles. Their work is inspired by the behavioral strategies of flying insects and is successfully demonstrated with a flying wing aircraft. Another more technically inspired approach in using optical flow measurements was presented

by the authors of [18]. They use a framework consisting of three nested Kalman filters and a quadrocopter for verification. Correspondingly, feature based vision systems are used by [9] to stabilize a quadrotor UAV or by [6] for position estimation using geo-referenced satellite or aerial images.

So far the described methods are less suitable for indoor navigation. Usually indoor scenarios have less textured surfaces to reliably detect optical flow or stable features. Laser scanners could be used as an alternative sensor. This for example is shown in [10].

The authors of [10] use a Hokuyo URG laser scanner on board a self made quadrotor UAV. The focus of their work was to transfer localization and mapping capabilities of ground vehicles to the UAV by using identical algorithms. With respect to the additional degree of freedom in translation, they use a mirror to deflect some of the laser rays towards the ground. A similar sensor configuration is used in [13] for path planning in information space. The objective is to find a path with good sensor measurements for robust localization. In contrast to [10] their UAV is a commercially produced *Hummingbird* quadrotor.

While the mentioned authors present working prototypes, one major drawback remains. Using the Hokuyo laser scanner results in a significant consumption of payload which constrains the possibilities to extend the system by additional sensors or computing power. Furthermore, the system's possible operation time will decrease. The authors of [1] compensate this problem by building a more powerful UAV. Their quadrotor is specially designed for carrying a stereo camera, a Hokuyo laser scanner with $30m$ range and a $1GHz$ Intel PC. However, the high payload of about $500g$ is traded for a shorter flight time of about 10 minutes.

We argue that the use of a laser scanner is not feasible, because it uses too much payload and the gathered 2D measurements are hard to use for 3D obstacle avoidance. However, obstacle detection is possible by using a stereo camera system, as shown in [1], but it depends on a structured and sufficiently illuminated environment to collect reliable measurements.

Using an active stereo system is our proposal for solving the issues. A combination of projecting a dot matrix of laser points and a laser line would give information about obstacles in flight direction through the laser points and more dense measurements from the laser line for localization or even a SLAM system.

The idea of obstacle avoidance with the help of a laser dot matrix is used for example in [21], where the authors developed a micro-inspector spacecraft for inspection of a host-vehicle.

Another group used a laser line projection combined with a camera to measure distances in [15] and [14]. They wanted to use their active stereo camera to aid people who suffer visual impairments and for obstacle detection in front of a driving car.

The authors of [12] are using a small amount of laser pointers for 3D reconstruction of a small room. Instead of linking the light source and the camera together, they use the laser pointers like a brush and move them across the scene while keeping the camera fixed.

III. Active Stereo System

A. Terminology

For reasons of clarity we want to explain the term *active stereo system* because it is used inconsistently in the literature: The authors in [25] and [17] use the term to describe a *single* camera supplemented by a structured light source. This is the same layout we describe in our paper. Such systems are referred to as being *active*, because in contrast to usual camera systems, they actively emit light into the environment. As the light source can be understood to be a virtual camera, we can still describe these systems as *stereo* systems.

In contrast to the above definition, the authors in [7] and [26] describe an active stereo system to consist of a common *stereo* camera and an additional non-uniform light source. The latter is used to generate texture upon weakly textured objects to simplify the stereo correspondence problem.

Other authors understand an active stereo system to consist of two cameras that can be panned or tilted independently, as in [19].

B. Introduction

In general we use the term *active stereo system* to describe a non-contact 3D measurement system which at least consists of one light projector and a camera. Widespread applications for active stereo systems are industrial 3D measurement or reconstruction tasks. A short summary of various systems with references to additional literature is given in [25]. Besides a short description of different light patterns, a variety of methods for calibration of such systems is given.

Active stereo systems can be most beneficially applied in indoor scenarios. Specifically, there is no need to find correspondences between two pictures like in passive stereo systems which is hard to achieve in rooms with monochromatic or low-textured walls. Moreover, the active stereo system is less dependent on well illuminated environments, which is advantageous because insufficient illumination could lead to blurred images in passive stereo systems due to the UAV's motion. In addition, the active stereo system will also work in complete darkness.

For the use on board a quadrotor UAV the light projector should be some kind of laser diode for reasons of size and weight. Generating a structured light pattern is for example possible by using a cylindrical lens for line generation or a *diffractive optical element* (DOE) for generating a grid of laser dots. Of course other patterns are possible, but these are the ones of interest for our work. In addition to the light source, we need a camera which we can use for both, live view for an operator and finding the light pattern for distance measurements.

C. Theory of Operation

Because we are using two active stereo system configurations, this section is divided into two parts. The first one

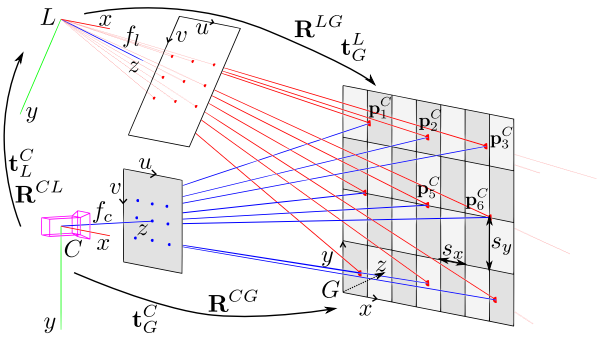

Fig. 2. Schematic view of an active stereo system with laser dot projection. In the upper left the laser is illustrated as a virtual camera, in the lower left a camera is shown and the calibration grid is displayed at the right side.

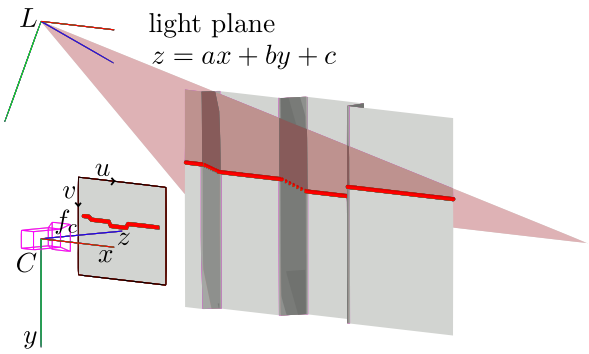

Fig. 3. Schematic view of an active stereo system with laser line projection. The laser emitting a plane of light is illustrated in the upper left side and the camera is shown as a pinhole model in the lower left position including its image frame. After intersection with an obstacle, the plane of light is transformed into a line.

will describe the combination of a camera and the laser generating the dot matrix structure, which is displayed in Fig. 2. The second part explains the theory for 3D reconstruction while using a laser line as light source in combination with a camera. This configuration is shown in Fig. 3.

1) Laser dot matrix: In the previous section, we saw that active stereo systems consist of a camera and a light source for generating a pattern. Analogous to conventional stereo cameras, both components will be arranged in a certain distance to each other, called baseline. Alongside with camera resolution and focal length, it mainly influences the possible distance resolution and therefore the measurement range of the system. Distance measurements can be achieved by triangulation which will result in distance-dependent resolutions as shown in Fig. 4(a). The diagram shows the relation between the disparity and the resulting range measurement of our prototype, based on the following equation:

$$u\,(z) = f\frac{B}{z} \tag{1}$$

Here, u is the disparity in pixels, f the focal length in pixels, B the baseline in meters, and z the distance in meters.

Figure 2 shows the two devices involved in the triangulation process of the described system. The camera and the

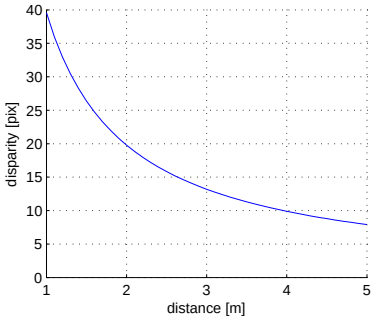

(a) Disparity

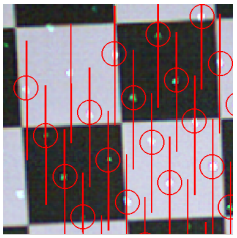

(b) Epipolar lines

Fig. 4. Disparity (a) and epipolar lines (b) of laser dot matrix and camera combination. The epipolar lines are shown as red lines and the position of detected laser dots as red circles.

laser generating a square laser dot matrix of three by three dots. Both components are shown with their local frame labeled L for the laser and C for the camera, which is modeled as a pinhole camera with focal length f_c. The position and orientation describing the relation between camera and laser is labeled $\mathbf{t}_L^C$ and $\mathbf{R}^{CL}$, where $\mathbf{t}_L^C$ stands for the translation of the laser frame given in the camera frame.

Starting in L, rays of light are emitted and projected upon an obstacle. In the case at hand, the obstacle hit is a plane checkerboard calibration grid, where the ray's intersections are shown as dots labeled $\mathbf{p}_i^C$. These dots are projected on the camera's image plane. Based on the position of a projected dot, the 3D position can be reconstructed. Analogous to stereo camera systems, each projected point will move along an epipolar line. By defining a lower and upper range of operation, the area in which a laser dot can be found is limited to a line in the image frame. An example is shown in Fig. 4(b). Depending on the location of the found laser point along the line, a different range measurement will be computed.

It is easy to see that a distinct assignment of a detected laser dot to the specific laser ray of the dot matrix is only possible if the grid is rotated slightly around its viewing direction. Without rotation, the epipolar lines will overlap, which will complicate the unique correspondence of a detected point to a ray of light. A more detailed description of the problem can be found in [21].

2) Laser line: Besides the dot matrix, there are other possible light patterns like a line of light which can be described as a plane of light located in the camera frame. Depending on the extrinsic parameters of such an active stereo system, the projected laser line will translate along a specific direction within the image when changing the distance to an object. A reasonable configuration for our application would be a vertical arrangement of the camera and the laser line generator as can be seen in Fig. 3. By choosing a horizontal orientation of the laser line, the resulting distance measurements will be generated for each column of the image by finding the position of the line. Basis for the distance computation is the following equation [16]:

$$\mathbf{p}^C = \frac{-c}{(a\,(u - c_u) + b\,(v - c_v) - f)} \cdot \begin{pmatrix} u \\ v \\ f \end{pmatrix} \qquad (2)$$

Where a, b and c are parameters of the light plane $z = ax + by + c$. The focal length is denoted f, u and v are the image coordinates, c_u and c_v label the image center coordinates and $\mathbf{p}^C$ is the resulting 3D point within the camera frame C.

D. Prototype

After discussing theoretical aspects of active stereo systems, we will continue with the description of our assembled prototype. As an imaging component we used an IDS uEye color camera with a resolution of 752x480 and 60 degrees horizontal field of view (FOV). For the structured light projection we mounted a sleeve at $6cm$ distance for clamping in a laser pointer either with point grid generation or line projection. For the first variant we used a low-cost laser pointer for about 15 € with $532nm$ wave length and integrated grating. The second combination consists of a camera and a low-cost laser with $650nm$ wave length, $5mW$ output power, and a cylindrical lens to generate a line with 90 degrees fan angle. This version can be seen in Fig. 1.

Both active stereo system combinations ensure an eye-safe operation, because of a low output power. Unfortunately they are unsuitable for operation in bright illuminated rooms. Therefore, we plan to use pulsed lasers linked to camera exposure in later prototypes. The authors of [14] discuss the amount of output power to guarantee eye-safety.

E. Calibration

For getting useful measurements, a calibration of the prototypes is required. Below we will give an outline of our calibration procedure, starting with the laser dot matrix system (Fig. 2), assuming an already calibrated camera.

1) Laser dot matrix: We computed the extrinsic parameters $\mathbf{R}^{CL}$ and $\mathbf{t}_L^C$ by using the algorithms of the well known *Matlab Camera Calibration Toolbox* [4] and consider the laser L to be a camera. This is done by the following approach: At first we take a picture of a checkerboard calibration pattern G with the projected laser points upon. Afterwards the user has to mark the outline of the checkerboard so that we can compute the plane orientation $\mathbf{R}^{CG}$ and translation $\mathbf{t}_G^C$ inside the camera frame. In the next step the laser points are detected for reprojection into the camera frame, forming multiple rays. Along with the plane, intersection points $\mathbf{p}_i^C$ can be calculated, resulting in 3D points upon the calibration plane. Now we can use the *Camera Calibration Toolbox* to compute the translation $\mathbf{t}_L^C$ and orientation $\mathbf{R}^{CL}$ of the virtual laser camera L within the real camera frame C. The points used as virtual camera image are generated with knowledge about the inter-ray angles of the laser dot matrix.

To validate the calibration parameters and to get an indication of the accuracy, we simulated the active stereo system with the estimated extrinsic parameters and projected the results into an image we did not use during the calibration procedure. For projecting the laser ray collision points with the plane, we need to extract the plane orientation as done in the calibration procedure. Afterwards, the 3D positions of the laser points can be projected into the image with the help of the camera's intrinsic parameters. Finally a comparison between the simulated points and the points detected inside the image can be made. Exemplarily, we simulated a grid of 7 by 7 points of which 45 points were detected in the image (Fig. 4(b)). The result is a mean distance error of 0.77 pixels and a maximum error of 1.8 pixels.

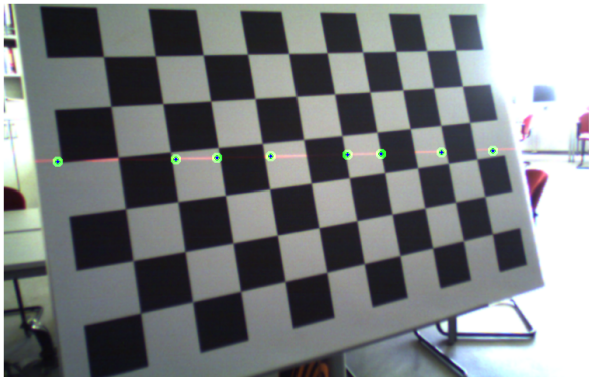

Fig. 5. Example of a calibration image showing the laser line, a calibration grid and user-selected dots.

2) Laser line: Consecutively, we can calibrate the active stereo system composed of camera and laser line projection. Here we need at least two images taken from different distances to the calibration pattern as basis to calculate the plane of light within the camera frame. In comparison to the former calibration scenario we do not need the exact position of the laser with respect to the camera. The equation of the light plane is sufficient to reconstruct the 3D points along the projected line.

To determine the light plane parameters, initially at least two images showing the calibration pattern and the laser line have to be collected. Afterwards the user manually chooses 8 points upon the line which will be approximated along a line using least squares to minimize the effect of inaccurate point selections. As before, a plane from checkerboard extraction step follows to calculate the 3D positions of the selected points. After repeating these two steps for all the collected images, the final parameters can be calculated. This is done by fitting all extracted 3D points onto a plane by using a least squares method. In addition, the 3D coordinates of the selected points can be derived with the new calibration parameters and compared to the ones calculated with the help of the calibration pattern. An example of such a calibration result is shown in Fig. 5.

F. Pattern Detection

1) Laser dot matrix: One critical step in acquiring range measurements is the detection of the light pattern within the image. In our first combination of camera and structured

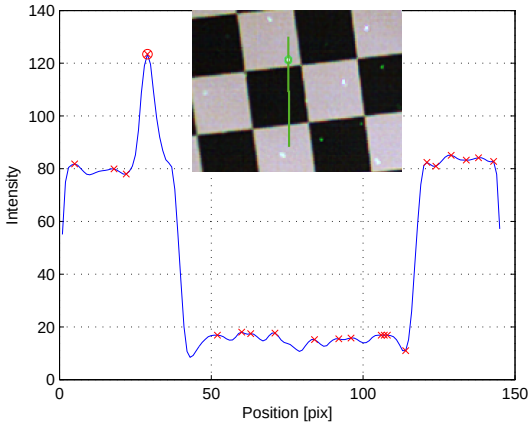

Fig. 6. Point detection along the epipolar line. The graph shows the smoothed intensity values along the line with local maxima indicated as crosses and the detected dot as a circle.

light source, the pattern is a green dot matrix generated by a $532nm$ laser pointer with grating. To detect the projected points we used a very simple algorithm. Operating on the green image channel along each epipolar line, we smoothed the intensities, then the first derivative is used to find all intensity maxima which are further examined regarding the slope before and after the maxima. If the absolute value of one slope is below a certain threshold, the maxima is discarded. This can occur for example in the transition of dark to light colors along a line through the checkerboard pattern. The intensities would result in a step with big slope on one side only. An example for the described procedure can be found in Fig. 6 which shows the intensity values along the line and local maxima found upon the line. Only the red circled maxima meets the conditions.

2) Laser line: The procedure for point detection can also be applied to line detection. In this case the red image channel is used because the line laser has a wavelength of $650nm$. Another modification concerns the search area. It is changed from the epipolar lines of the points into the vertical rows of image pixels. Furthermore, we assume a room with partially straight walls so that we group the detected points into line segments to avoid noise in the line detection. To accomplish the grouping we use the well known split-and-merge algorithm as for instance described in [24]. In addition, each set of grouped points could be fitted onto a line by least squares optimization, but this resulted in unwanted leaps within the distance measurements.

IV. Simulated Proof of Concept

For proving our measurement concept we used the USARSim simulation environment [5]. Therefore, we extended the simulation with two new sensors based on range measurements. One sensor is generating range measurements based on the dot matrix light pattern and the other one is generating range measurements based on a laser line. The combination is shown as an onboard camera image in Fig. 7, which is captured with our modified image server [8].

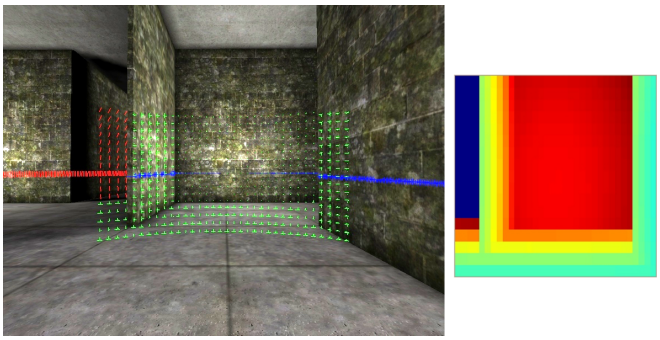

Fig. 7. The left image shows the new USARSim sensor models with activated debug information. Red marks are out of range, green are valid measurements for the laser grid based sensor and blue are the valid measurements for the laser line based sensor. On the right image, the acquired depth measurements of the laser grid based sensor are shown as a colored depth map.

The green and blue crosses are showing the intersection points between obstacles and the simulated laser rays of our new sensors. They are drawn directly into the simulation environment with the help of debug lines, due to lack of adequate API functions.

Currently the simulation generates exact distance measurements, because realistic noise effects of the active stereo system are hard to simulate. In reality there may be errors as a consequence of the camera calibration procedure, or because of the approximated extrinsic parameters from the active stereo system calibration. Even without realistic noise models, the simulation is useful for validating control strategies, mapping algorithms, or the interpretation of measurements. Furthermore, a reactive obstacle detection can be implemented and easily tested without damaging the UAV.

V. Real World Experiments

In this section we present some measurements acquired by our laser line prototype. Our objective is to generate accurate position estimations with the laser line prototype to perform a rough 3D environment reconstruction with the additional laser dot matrix in later work. Therefore, we concentrate our efforts on the validation of the laser line prototype in combination with a specific mapping application. In case of exact measurements, we would expect that we can use our range measurements acquired by the active stereo system as input for an ICP (Iterative Closest Points) based localization system as well as for an ICP-SLAM system. To validate our ideas, we used the *Mobile Robot Programming Toolkit (MRPT)* [3] which includes an ICP algorithm, different SLAM applications and other useful tools to handle the acquired measurements.

The ICP algorithm used in MRPT is described in [22]. Its main characteristic is the adaptive outlier detection which distinguishes the algorithm from other implementations. Based on a progressively decreasing threshold in each iteration of the ICP error minimization step, the maximum distance error allowed for inclusion of a point match is adapted. The algorithm is able to match two point maps, like

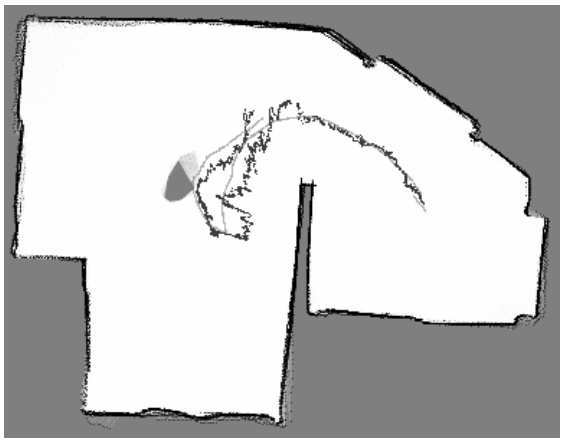

Fig. 8. Occupancy grid map generated by the ICP-SLAM application based on measurements of the Hokuyo laser range finder. In the localization experiment the map is used as reference for position estimation. The bright grey path shows the results of the localization experiment based upon the Hokuyo measurements and the dark path shows the calculated positions based upon the active stereo camera system measurements.

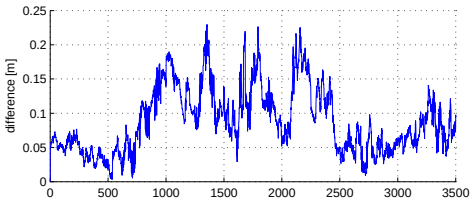

(a) Distance error

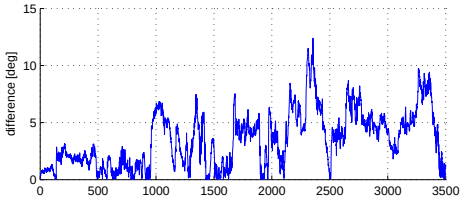

(b) Orientation error

Fig. 9. Resulting errors in pose based on Hokuyo laser scan data as ground truth.

two different laser scans, or a point map with an occupancy grid map. The later case is used in the ICP-SLAM application to build a global occupancy grid map out of the separate laser scans.

For our experiments, we used a mobile platform without any internal sensors and only mounted an Hokuyo laser scanner and the active stereo system with the laser line projector on it. The Hokuyo laser scanner is only used for comparing the results with our active stereo system so we can determine the achieved accuracy of the system. The environment in which we collected the measurements was a room with a size of about 3 by 4 meters.

A. Localization within an Occupancy Grid Map

Our goal is to determine our position and orientation within a previously known map. Therefore, we apply the widely used ICP algorithm, which aligns two metric maps by minimizing the point distances using least squares optimization. In the case at hand, the optimization is done between consecutive measurements and an occupancy grid map, which was built earlier using the Hokuyo laser scan measurements. The map is shown in Fig. 8.

A dataset with synchronously acquired active stereo system measurements and Hokuyo laser scan data is used as input for two separate ICP runs. We consider the localization results of the pose tracking with the Hokuyo laser scanner as ground truth and compare them with the results based upon the active stereo system. The calculated positions within the map can be seen in Fig. 8 as two separate paths. Position and orientation errors are shown in Fig. 9(a) and 9(b) yielding a mean distance error of about 0.09 meters with a standard deviation of 0.05 meters in the position measurements and a mean orientation error of 3.5 degrees with a standard deviation of 2.4 degrees.

B. ICP-SLAM

In our second experiment we use the sensor data not only for localization, but also for mapping of the environment. Therefore, we used an ICP-SLAM system with the same data as before, but without a previously known map. The measurements were now used for both, building the occupancy grid map of all previous measurements and localization within this map based on the current measurement.

At first, we used the acquired laser scan measurements as input for the ICP-SLAM application. As expected, the accurate measurements lead to an adequate reconstruction of the room's layout. The result can be seen in Fig. 10(b). Afterwards, we took the synchronously acquired measurements of the active stereo system as input data. As can be seen in Fig. 10(a), the results are not as good as with the Hokuyo laser scanner. A connected wall was generated, but not in the right angles among the piecewise straight wall segments and in a outwards curved way.

C. Error Analysis

There are several possible reasons for the unexpected result of the active stereo system. Inaccurate measurements appear mainly in outer image regions, so they may be corrected with better calibration and a more optimized line extraction algorithm.

The usage of a color camera in combination with a red laser induces another source of inaccuracy. For sensing color, the CCD chip within the camera is combined with color filters for red, green, and blue on each sensor element, which is known as bayer pattern. Each pixel in the color image is a result of four combined sensor elements of the colors red, blue and two times of green. So the effective resolution of the red image channel which is used for the detection of the laser line is only 25 percent of the camera resolution. This has an impact on the achievable range resolution of the active stereo system.

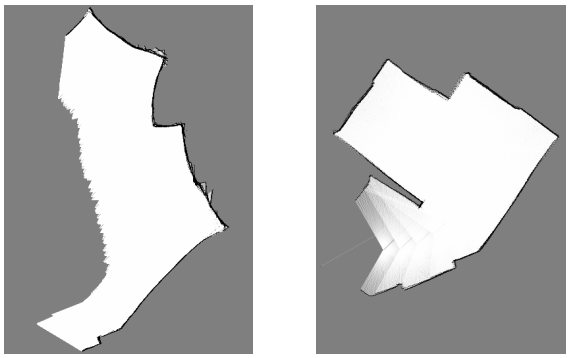

(a) Active stereo (b) Hokuyo

Fig. 10. Occupancy grid maps generated by the ICP-SLAM algorithm.

Compared to the Hokuyo measurements, the active stereo system provides less measurements and measurements with increasing noise in larger distances. This has negative effects on the used ICP algorithm, since it is commonly used and optimized for laser scan measurements which have almost a constant noise within the whole sensor range. Distant point matches are weighted and used in the same way as point matches within a shorter range to the sensor. Since distant points are more likely to be inaccurate, the resulting ICP position and orientation estimation is more error-prone compared to laser range finder measurements.

Another advantage of the Hokuyo laser range finder is its field of view of 240 degrees which is four times larger than the FOV of the active stereo system. Depending on distinct features, a higher FOV results in a lower possibility of reaching a wrong local minimum within the ICP algorithm. So it is more likely that the ICP algorithm runs into a wrong translation and orientation by using the active stereo system measurements.

VI. Conclusions and Further Work

We could prove the feasibility of the structured light measurement system. The achieved results support our idea of using it on board a quadrotor UAV. Additional work needs to be done regarding calibration, line detection and also the choice of the used hardware to accomplish a working SLAM system. We plan to combine the two different light sources with green laser dots and the red laser line to acquire 3D measurements for both light sources simultaneously to get accurate position estimates and generate a rough reconstruction of the environment in 3D.

We will evaluate the implementation of a more realistic active stereo camera system in the simulation environment to eliminate sources of error induced by the used hardware. This is necessary for further development of the ICP-SLAM system. A concept of generating the laser line in USARSim using the debug functions of the underlying Unreal Engine has already been tested successfully.

Further research will be done regarding the used ICP-SLAM system, which should consider the increasing uncertainty in larger distances. Therefore, we plan to implement an ICP variant which incorporates the sensor's position uncertainty and the range dependent measurement uncertainty.

References

[1] Markus Achtelik, Abraham Bachrach, Ruijie He, Samuel Prentice, and Nicholas Roy. Autonomous Navigation and Exploration of a Quadrotor Helicopter in GPS-denied Indoor Environments. In *First Symposium on Indoor Flight Issues*, 2009.

[2] Antoine Beyeler, Jean-Christophe Zufferey, and Dario Floreano. Vision-based control of near-obstacle flight. *Autonomous Robots*, 27(3):201–219, 2009.

[3] José-Luis Blanco. The Mobile Robot Programming Toolkit (MRPT). `http://www.mrpt.org`, Apr. 2010.

[4] Jean-Yves Bouguet. Camera Calibration Toolbox for Matlab. Website, 2009. Available online at `http://vision.caltech.edu/bouguetj/calib_doc`.

[5] Stefano Carpin, Michael Lewis, Jijun Wang, Stephen Balakirsky, and Chris Scrapper. USARSim: a robot simulator for research and education. In *Proc. of IEEE International Conference on Robotics and Automation, ICRA07*, pages 1400–1405, Roma, Italy, April 2007.

[6] G. Conte and P. Doherty. An Integrated UAV Navigation System Based on Aerial Image Matching. In *Aerospace Conference, 2008 IEEE*, pages 1–10, 2008.

[7] J. Diebel, K. Reutersward, S. Thrun, J. Davis, and R. Gupta. Simultaneous Localization and Mapping with Active Stereo Vision. In *Proc. of the IEEE/RSJ International Conference on Intelligent Robots and Systems, IROS04*, volume 4, pages 3436–3443, 2004.

[8] Sebastian Drews. Image Server. Website, 2010. Available at `http://www.tu-chemnitz.de/etit/proaut/forschung/simulation.html.en`.

[9] Spencer G. Fowers, Dah-Jye Lee, Beau J. Tippetts, Kirt D. Lillywhite, Aaron W. Dennis, and James K. Archibald. Vision Aided Stabilization and the Development of a Quad-Rotor Micro UAV. In *Proc. of the International Symposium on Computational Intelligence in Robotics and Automation, CIRA07*, pages 143–148, 2007.

[10] Slawomir Grzonka, Giorgio Grisetti, and Wolfram Burgard. Towards a Navigation System for Autonomous Indoor Flying. In *Proc. IEEE International Conference on Robotics and Automation, ICRA09*, Kobe, Japan, 2009.

[11] Daniel Gurdan, Jan Stumpf, Michael Achtelik, Klaus-Michael Doth, Gerd Hirzinger, and Daniela Rus. Energy-efficient Autonomous Four-rotor Flying Robot Controlled at 1 kHz. In *Proc. of IEEE International Conference on Robotics and Automation, ICRA07*, Rome, Italy, April 2007.

[12] Martin Habbecke and Leif Kobbelt. LaserBrush: A Flexible Device for 3D Reconstruction of Indoor Scenes. In *Proc. of the 2008 ACM Symposium on Solid and Physical Modeling, SPM08*, pages 231–239, New York, NY, USA, 2008.

[13] Ruijie He, Sam Prentice, and Nicholas Roy. Planning in Information Space for a Quadrotor Helicopter in a GPS-denied Environments. In *Proc. of the IEEE International Conference on Robotics and Automation, ICRA08*, pages 1814–1820, Los Angeles, CA, 2008.

[14] David Ilstrup and Gabriel Hugh Elkaim. Low Cost, Low Power Structured Light Based Obstacle Detection. In *ION/IEEE Position, Location, and Navigation Symposium, ION/IEEE PLANS08*, pages 865–870, Monterey, CA, 2008.

[15] David Ilstrup and Gabriel Hugh Elkaim. Single Frame Processing for Structured Light Based Obstacle Detection. In *ION National Technical Meeting, ION NTM 2008*, San Diego, CA, 2008.

[16] X. Jiang and H. Bunke. *Dreidimensionales Computersehen - Gewinnung und Analyse von Tiefenbildern*. Springer, 1996.

[17] Hiroshi Kawasaki, Yutaka Ohsawa, Ryo Furukawa, and Yasuaki Nakamura. Dense 3D Reconstruction with an Uncalibrated Active Stereo System. In *Proc. on the 7th Asian Conference on Computer Vision, ACCV06, Part II*, pages 882–891, 2006.

[18] Farid Kendoul, Isabelle Fantoni, and Kenzo Nonami. Optic flow-based vision system for autonomous 3D localization and control of small aerial vehicles. *Robotics and Autonomous Systems*, 57(6-7):591–602, 2009.

[19] Hyukseong Kwon, Johnny Park, and Avinash C. Kak. A New Approach for Active Stereo Camera Calibration. In *Proc. of IEEE International Conference on Robotics and Automation, ICRA07*, pages 3180–3185, 2007.

[20] Sven Lange, Niko Sünderhauf, and Peter Protzel. A Vision Based Onboard Approach for Landing and Position Control of an Autonomous Multirotor UAV in GPS-Denied Environments. In *Proc. of the International Conference on Advanced Robotics, ICAR09*, Munich, Germany, 2009.

[21] Carl Christian Liebe, Curtis Padgett, Jacob Chapsky, Daniel Wilson, Kenneth Brown, Sergei Jerebets, Hannah Goldberg, and Jeffrey Schroeder. Spacecraft Hazard Avoidance Utilizing Structured Light. In *IEEE Aerospace Conference*, Big Sky, Montana, 2006.

[22] Jorge L. Martínez, Javier González, Jesús Morales, Anthony Mandow, and Alfonso García-Cerezo. Mobile Robot Motion Estimation by 2D Scan Matching with Genetic and Iterative Closest Point Algorithms. *J. Field Robotics*, 23(1):21–34, 2006.

[23] MikroKopter. Website, 2010. Available online at `http://www.mikrokopter.com`.

[24] Viet Nguyen, Agostino Martinelli, Nicola Tomatis, and Roland Siegwart. A Comparison of Line Extraction Algorithms using 2D Laser Rangefinder for Indoor Mobile Robotics. In *Proc. of the IEEE/RSJ Intenational Conference on Intelligent Robots and Systems, IROS05*, Edmonton, Canada, 2005. IEEE.

[25] M. Ribo and M. Brandner. State of the Art on Vision-Based Structured Light Systems for 3D Measurements. *International Workshop on Robotic and Sensor Environments, ROSE05*, pages 2–6, October 2005.

[26] D. Viejo, J.M. Saez, M.A. Cazorla, and F. Escolano. Active Stereo Based Compact Mapping. In *Proc. of the IEEE/RSJ International Conference on Intelligent Robots and Systems, IROS05*, pages 529–534, 2005.